Online ISSN 1848-3380, Print ISSN 0005-1144
ATKAFF 57(4), 948–959(2016)

Abdelhakim Mabrek, Kamel E. Hemsas

Induction motor inter-turn fault modeling and simulation using SSFR test for diagnosis purpose

DOI 10.7305/automatika.2017.10.1805
UDK 681.518.54:621.313.333

Original scientific paper

This paper presents a new idea to establish a simplified model of the short-circuit turns (SCT), in the stator winding of the squirrel-cage induction motor (IM) using standstill frequency response test (SSFR). This method may offer more precision in parameters estimation independent of variations in motor or load operating conditions since it is at standstill test. However, high-performance field-oriented control, or diagnosis purpose of the IM requires accurate knowledge of the electrical parameters. Furthermore, we propose to model the IM by a multiple cage equivalent circuit (EC) that enables us to take into account the deep bar effect with accuracy.

The specific advantage of the proposed method that we can create a true SCT at several levels using fault simulator in order to estimate the EC model parameters in each case of fault severity, with a low probability of risk to the machine being tested, and a relatively modest expense.

At the first time the healthy machine is identified and experimentally validated, then the models have been successfully used to study the transient and steady-state behavior of the IM with SCT fault, which a practically oriented scientific value.

Key words: Diagnosis, Induction motor, Parameter identification, Short-turns, Spectrum, Standstill

Modeliranje i simulacija međuzavojskog kvara asinkronog motora upotrebom SSFR testa za dijagnostičke svrhe. U radu je predstavljena nova ideja za uspostavljanje pojednostavljenog modela kratkospojenih zavoja (SCT) u namotu statora kaveznog asinkronog motora (IM) upotrebom testa frekevencijskog odziva u mirovanju (SSFR). Ova metoda moguće pruža precizniju procjenu parametara neovisno o varijaciji motorskih ili teretnih radnih uvjeta jer se testiranje provodi u mirovanju. Ipak, vektorsko upravljanje visokih performansi ili dijagnostička IM-a zahtijevaju točno poznavanje električkih parametara. Nadalje, predlažemo model IM-a s višekaveznom nadomjesnom shemom (EC) koja nam omogućuje da u obzir uzmemo točan efekt duboko pozicioniranih kaveznih štapova. Posebna prednost predložene metode je što možemo načiniti vjerodostojni SCT model na nekoliko razina upotrebom simulatora kvara da bismo procjenili parametre EC modela u različitim stadijima kvara, s malom vjerojatnosti rizika za korišteni stroj te relativno umjerene troškove. Prvo se identificira i eksperimentalno provjeri neoštećeni stroj, a zatim se modeli uspješno koriste za proučavanje dinamičkog i stacionarnog ponašanja IM-a s SCT kvarom što posjeduje praktično-orijentiranu znanstvenu vrijednost.

Ključne riječi: Dijagnostika, asinkroni motor, identifikacija parametara, kratki spojevi, spektar, mirovanje

1 INTRODUCTION

Induction motors are the most commonly used in electrical drives, because it has been playing a non-substitutable role in a variety of diverse industries and received augmented attention owing to their robust construction, reliability, lower initial, maintenance cost and high performance. Any kind of faults on induction machines may yield drastic consequences that can lead to motor interruption if left undetected, and their resulting unplanned downtime is very costly. It is well known that fault detection in IM at an early stage may not only minimize breakdowns and reduce maintenance time, but also stops propagation of the fault or limit their increase to severe degrees, the reason for such faults may reside in small errors during motor manufacturing [1].

Several reported works show that 30% at 40% of IM failures are due to stator windings breakdown [2]. Moreover, most of these faults start as an inter-turn short circuit in one of the stator winding, high circulating currents are induced in short circuit turns where the related produced heating can damage the winding's insulation [3]. Therefore, stator fault diagnosis has received intense research interest. In recent years, many research works have been carried out on the monitoring condition and diagnosis of elec-

trical machines [4]. Many tools of calculation have been proposed for electrical machine faults detection and localization. These tools are based on spectral analysis of stator current voltage, torque, external magnetic flux density, and vibration. And it had been shown that current monitoring can be used to estimate stator insulation degradation [5].

Recently, continuous identification has been used to perform the diagnosis procedure. These techniques study the deviation of parameters using experimental tests to detect and localize faults. Some paper presents a new diagnosis technique of squirrel-cage IM's by off-line parameter identification using real data. It is necessary to work in a continuous time representation because all parameters have physical significance (resistance, inductance), it is important to introduce this physical knowledge to perform parameter estimation for diagnosis purpose, thus parameter estimation with prior information offers an elegant solution [6-7-8].

Other researchers provide a method for detecting the rotor anomalies in IM using standstill tests [9-10-11]. Each one demonstrates that using standstill tests instead of rotating ones because they avoid the inherent influence of the slip in the stator current and flux measurements.

Moreover, this technique is very easy to implement with low-cost instruments. Furthermore, it's more difficult to create a real fault into the machine at nominal voltage and monitor their effects on the machine characteristics to study the behavior of the machine under fault conditions, this is because the fault can be dangerous for the motor and can lead to the destruction of the machine. For this reason, the modeling of IM remains always an effective tool to study the effect of faults on motor performance. So it had been the first step in the design of turn fault detection systems, simulation of transient and steady state behavior of motors with these models enable correct evaluation of the measured data by diagnostic techniques [12-13-14].

In the modeling of internal faults of electric machines two approaches stand out, namely the winding-function-based approach, and the time stepping finite-element-based approach [15-16]. In this paper, the SSFR analysis is used for determining the proposed EC model parameters of the healthy IM. Then, the proposed model is used for studying the machine behavior under the healthy state condition using MATLAB-Simulink software. The IM under inter-turn fault is also modeled and studied by SSFR analysis. Finally, the comparison of the results of the faulty model simulation and experimental results allowed verifying the precision of the proposed model for different levels of fault severity.

2 STATE OF ART AND METHODOLOGIES OF THE WORK

The paper presents an experimental verification of previously established EC machine model for comprehending inter-turn faults scenario, the specific advantage of the proposed method that we can create a real fault into the IM using faults simulator, to extract model parameters of faulty motors with a low probability of risk and relatively modest expense. Then the model has been successfully used to study the transient and study state behavior of the IM with SCT fault which a practically-oriented scientific value.

The work performed was subdivided into three main steps as mentioned in Fig. 1.

a) SSFR analysis of the healthy motor and with the stator winding turn faults, to carry out all needed stator and rotor parameters of EC at standstill.

b) Matlab simulator building, by using the EC phase model of the induction motor at healthy and faulty state, to study the behavior of the motor.

c) Experimental validation and fast Fourier transform analysis (FFT) of the stator current, in order to validate the SCT model derived from SSFR test by comparison with the research results presented before.

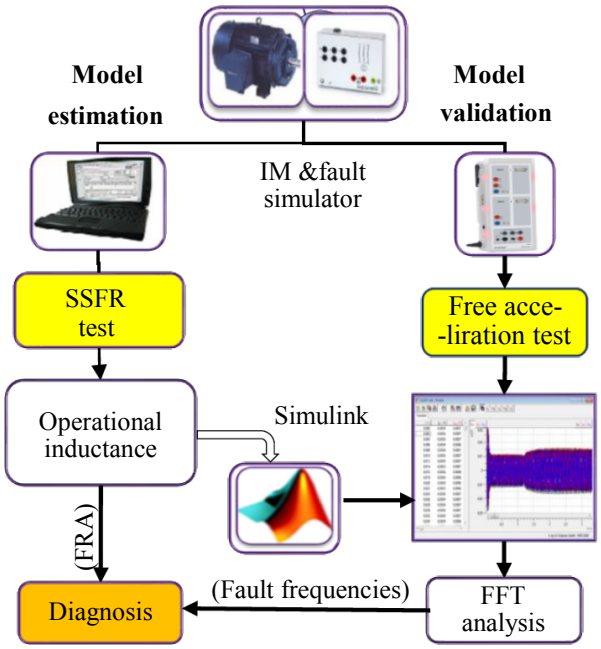

Fig. 1. Research plan (induction motor identification and validation scheme)

3 MODELING OF INDUCTION MOTOR AT STANDSTILL IN FREQUENCY DOMAIN

SCT faults of the IM yield to high levels of stress in an induction traction drive. To study these operations, the IM had been modeled by a multiple cage EC. This enables us to take into account the deep bar effect with accuracy. The mathematical model of an IM with *N* equivalent rotor circuit can be described by the nonlinear differential equation (1). To study the transient operations of the IM, an operational formulation of the electrical equations is often used. This formulation is obtained by substitution of derivative operator d/dt by the Laplace operator *p*, (Adkins and Harley, 1975).

$$\begin{cases} \overrightarrow{V_s} = R_s \overrightarrow{I_s} + \frac{d\overrightarrow{\psi}_s}{dt} \\ \overrightarrow{0} = R_{r(j=1,\ N)} \overrightarrow{I}_{r\ (j=1,N)} + \frac{d\overrightarrow{\psi}_{r_{(j=1,N)}}}{dt} - \\ \quad -j\omega_r(\overrightarrow{\psi}_{(j=1,\ N)}) \end{cases}, \quad (1)$$

$$\begin{cases} V_s(p) = R_s I_s(p) + p\psi_s(p) \\ 0 = R_{rN} I_{rN}(p) + p\psi_{rN}(p) - j\omega_r \psi_{rN} \end{cases}. \quad (2)$$

To derive the transfer function of IM, we should transform (2) to a linear parametric model. So, consider the IM at standstill $\omega_r = 0$, we take $N = 2$:

$$\begin{cases} V_s(p) = R_s I_s(p) + p\psi_s(p) \\ 0 = R_{r1} I_{r1}(p) + p\psi_{r1}(p) \\ 0 = R_{r2} I_{r2}(p) + p\psi_{r2}(p) \end{cases}. \quad (3)$$

Then the flux, equations are given in (4):

$$\begin{cases} \psi_s(p) = L_m[I_{r1}(p) + I_{r2}(p)] + L_0 I_s(p) \\ \psi_{r1}(p) = L_m I_r(p) + L_{r1} I_{r1}(p) + L_m I_s(p) \\ \psi_{r2}(p) = L_m I_r(p) + L_{r2} I_{r2}(p) + L_m I_s(p) \end{cases}, \quad (4)$$

with

$$\begin{cases} L_0 = L_m + L_{\sigma s} \\ L_{r1} = L_m + L_{\sigma r1} \\ L_{r2} = L_m + L_{\sigma r2} \end{cases}. \quad (5)$$

The expression of the operational inductance can be obtained from (3) and (4) and is given by:

$$L_s(p) = L_0 \frac{\left(1 + pT^{'}\right)\left(1 + pT^{''}\right)}{\left(1 + pT_0^{'}\right)\left(1 + pT_0^{''}\right)}. \quad (6)$$

The open circuit and short circuit time constants of (6) are given respectively in (7):

$$\begin{cases} T_0^{'} = \frac{L_{\sigma r1} + L_m}{R_{r1}} \\ T^{'} = \frac{(L_{\sigma r1} + L_{\sigma s})}{R_{r1}} \end{cases}. \quad (7)$$

The sub-transient open circuit and sub-transient short circuit time constants of (6) are given respectively in (8):

$$\begin{cases} T_0^{''} = \frac{L_{\sigma r2} + (L_m // L_{\sigma r1})}{R_{r2}} \\ T^{''} = \frac{L_{r2} + (L_m // L_{\sigma r1} // L_{\sigma s})}{R_{\sigma r2}} \end{cases}. \quad (8)$$

The corresponding EC is presented in Fig. 2, it is usable for transient operations. And their parameters are given in Appendix A.

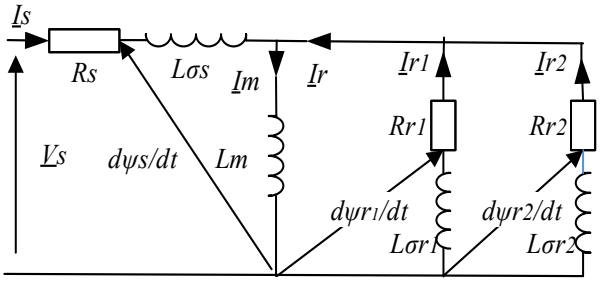

Fig. 2. EC model of IM at standstill

4 PARAMETERS IDENTIFICATION OF THE EQUIVALENT CIRCUIT MODEL OF IM

The procedure for determining the values of IM parameters using the frequency response test data follow three steps [17].

4.1 Step 1:

Firstly, the standstill frequency response test is performed to determine the data of operational impedance (OIM) and transfer functions, which punitively describe the interactions of voltages, and currents as functions of frequency as given in (9), where R_s is the stator resistance:

$$Z_s(j\omega) = \frac{V_s(j\omega)}{I_s(j\omega)} = R_s + j\omega L_s(j\omega). \quad (9)$$

From this frequency response of OIM, the frequency response of the operational inductance (OIN) can be determined in (10):

$$L_s(j\omega) = \frac{Z_s(j\omega) - R_s}{j\omega}. \quad (10)$$

4.2 Step 2:

Secondly, we determine the transfer function of the OIN to quantize the current-flux-voltage relations in simple standard forms as it demonstrated in (6), [17].

as data are continuous-time (frequency-domain) data, so authors used output-error (OE) technique to estimate a continuous-time model with a transfer function, OE

method based on the iterative minimization of an OE quadratic criterion by a nonlinear programming (NLP) algorithm. These techniques require much more computation and do not converge to a unique optimum. But, OE methods present very attractive features, because the simulation of the output model is based only on the knowledge of the input, so the parameter estimates are unbiased [6].

The transfer function of continuous-time estimated from real data is given in (11):

$$L_s(p) = \frac{b_{nb}p^{(nb-1)} + b_{(nb-1)}p^{(nb-2)} + \cdots + b_1}{p^{nf} + f_{nf}p^{(nf-1)} + \cdots + f_1}, \quad (11)$$

and the parameter vector θ estimated from this transfer function is:

$$\theta = \left\lfloor L_0,\ T^{'}, T^{''},\ T_0^{'},\ T_0^{''} \right\rfloor. \quad (12)$$

4.3 Step 3:

The parameters of the EC model shown in Fig. 2 are estimated from (6), using Canay's algorithm [19]. This one present a method need the passage, without approximation of time constants to generalized circuit parameters from (7) and (8).

5 APPLICATION OF THE SSFR TEST IN IDENTIFICATION OF SCT MODEL

5.1 Definition of SSFR method

An alternative procedure called standstill frequency response (SSFR) testing proposed in by the IEEE committee in 1983. Reports which cover the theoretical background, including Laplace, transform analysis of synchronous machines at standstill. Such responses describe the rates of change of various stator or field quantities over a range of sinusoidal excitations from very low frequencies up to and considerably beyond nominal values. In order to carry out these tests, the machine has to be at standstill before the impedance of the machine can be measured from machine stator terminal (Fig. 3). The process of measuring these impedances is done through the variation of the frequency signal applied to two winding and as this frequency is varied, the magnitude and phase of the input current are measured. With these measurements are taken, the parameters of the machine can then be determined [20].

5.2 Squirrel cage fault simulator

The fault simulator, in conjunction with asynchronous squirrel-cage motors allows for simulation of typical malfunctions like shorts to ground, winding breaks, turn-to-turn faults, winding -to-frame shorts and tripping of the thermal circuit breaker. The faults are generated by 13 switches ($S1, \ldots, S13$), arranged behind a locked cover. The fault simulator is an adapter to be attached to the terminal panel of the squirrel cage motor (Fig. 4).

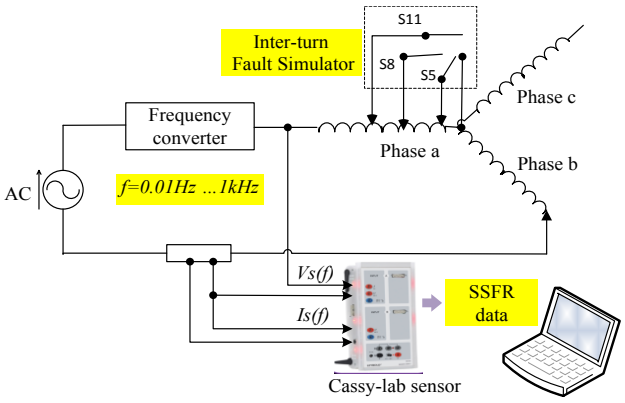

Fig. 3. IM testing at standstill with SCT fault

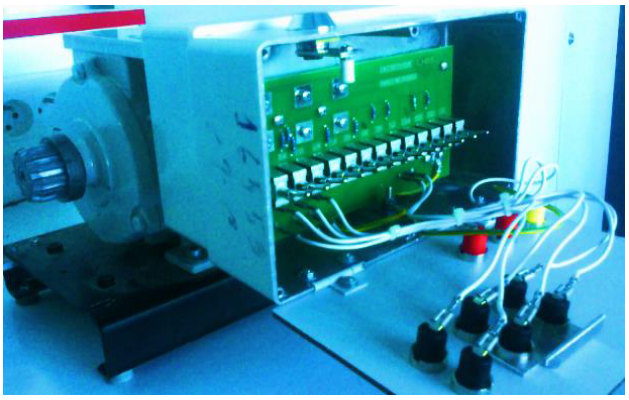

Fig. 4. Squirrel cage fault simulator

6 EXPERIMENTAL TEST

The main objective of this second part is to use the SSFR identification method to derive healthy and faulty IM models. This method consists of building different measurement of the operational inductance. The experimental data acquisition is made by (Cassy_Lab) system connected to the computer, for processing by the software Matlab. Over a frequency range (0.1 to 1 kHz), the frequency response analyzer measures the phasor- relationship between the current $I_s\ (j\omega)$, injected into the motor terminals and the corresponding voltage $V_s\ (j\omega)$ induced across the motor terminals [21].

The experimental unit, as shown in Fig. 5, includes:

- A variable industrial frequency power supply generates more than three decades, from about 0.1 Hz through to well over 1000 Hz and fixed voltage value.
- Induction motor 4-pole, 250 W, 400/230 V connected to the stator fault simulator.
- Personal computer with software CASSY_LAB.

- Sensor card Cassy_Lab.
- Power-amplifier.

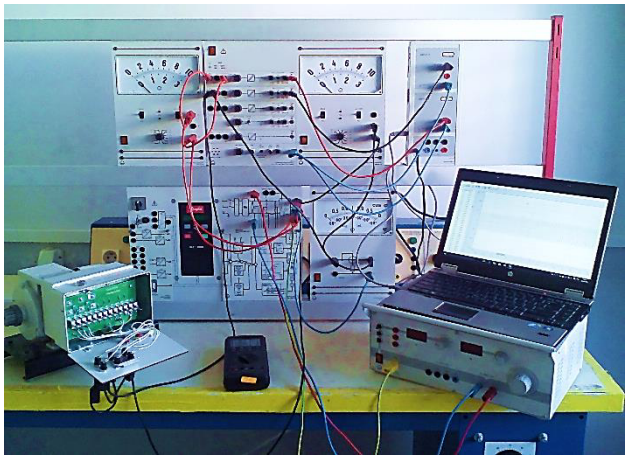

Fig. 5. Experimental bench for SSFR identification

6.1 Experimental identification results

The continues-time transfer functions of second order estimated from real dada in both healthy, and faulty scenario of IM are organized in Table 1.

An OE technique is used, and the search direction for minimizing criteria can be computed by adaptive Gauss-Newton method for final prediction error (FPE) minimization:

$$FPE = LF * (1 + 2 \cdot d/M), \tag{13}$$

where LF is the loss function, d is the number of estimated parameters and M is the number of estimation data samples, noted that $d << M$ is assumed.

Table 1. Estimated transfer functions of IM

	Continuous 2^{nd} order model	**FPE**
Healthy IM	$L_{s\ (health)} = 0.2229 \frac{(p+129.3)\ (p+3.425)}{(p+27.49)\ (p+2.477)}$	0.0114
Faulty 5%	$L_{s\ (sct\ 5\%)} = 0.2038 \frac{(p+131.7)\ (p+3.244)}{(p+25.45)\ (p+2.466)}$	0.0112
Faulty 20%	$L_{s\ (sct\ 20\%)} = 0.1569 \frac{(p+116.7)\ (p+2.52)}{(p+20.78)\ (p+2.03)}$	0.0040
Faulty 40%	$L_{s\ (sct\ 40\%)} = 0.1077 \frac{(p+131.8)\ (p+8.54)}{(p+33.32)\ (p+4.74)}$	0.0023

To obtain feasible transfer function of IM, the frequency responses are directly curve fitted using the measured SSFR data.

Once the OIN is calculated, standard bode techniques are used to determine a transfer function that will be tested in this project, a second order function for $L_s(p)$ as given in (6) was found to provide a good approximation to the test data.

Figure 6 shows that the 2nd order model given in Table 1 has obviously excellent agreement with the measurements in both healthy and faulty cases ($FPE \leq 0.01$). This attests the accuracy of the models and measured inductance operators.

Given this function, appropriate equivalent circuit parameters were calculated using software written for this purpose.

Table 2 shows the time constants (sec) and EC parameters, resistance (ohm), inductance (H), extracted from the continuous transfer functions in both healthy and faulty IM.

Table 2. Time constants and EC parameters

	Healthy IM	**Faulty 5%**	**Faulty 20%**	**Faulty 40%**
$\boldsymbol{T_0^{'}}$	0.2919	0.3082	0.3968	0.1170
$\boldsymbol{T_0^{''}}$	0.0077	0.0076	0.0086	0.0076
$\boldsymbol{T^{'}}$	0.4037	0.4056	0.4913	0.2107
$\boldsymbol{T^{''}}$	0.0364	0.0393	0.0481	0.0300
$\boldsymbol{R_s}$	45.662	43.859	37.313	27.548
$\mathbf{L}_{\sigma s}$	0.1988	0.1767	0.1446	0.0883
$\boldsymbol{L_m}$	1.2507	1.2109	0.9471	0.6792
$\boldsymbol{R_{r1}}$	10.723	12.1230	9.6744	8.0288
$\boldsymbol{R_{r2}}$	24.1967	23.1707	15.6403	12.202
$\boldsymbol{L_{r1}}$	2.96323	3.5857	3.71574	0.8657
$\boldsymbol{L_{r2}}$	0.02484	0.0280	0.01265	0.0205

6.2 Diagnosis and fault indicator

The main concept is to use SSFR test to observe the variation of equivalent impedance due to the SCT fault whenever the motor is stopped. It is shown that the decrease in the value of the OIN under standstill excitation can be used as an indicator of increasing in the number of shorted turns. The frequency response analysis (FRA) test could be used to detect and even to locate turn to turn and ground fault in rotating electrical machines, and especially in field windings [22]. Four tests have been carried out in order to verify that fault can be detected for different severity degree using FRA test, as presented in Fig. 6, the SCT fault has influence on the amplitude of the OIN. The fault can be clearly detected in the low-frequency range [0.1 -100 Hz], as the number of shorted turns increase the amplitude decrease, and the frequency response becomes minor if compared to the healthy IM, but has a small influence in the [100–10 kHz] frequency interval.

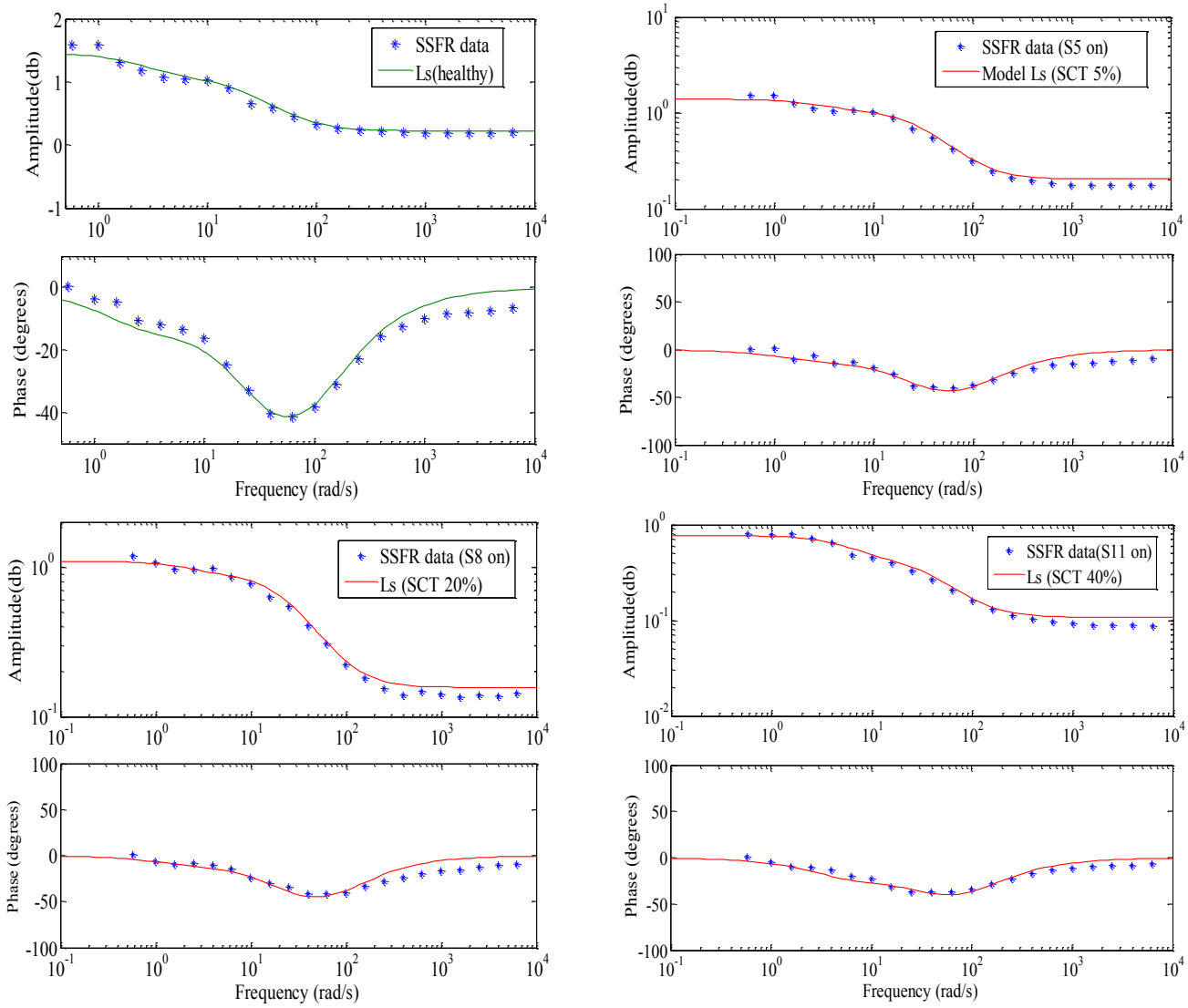

Fig. 6. OIN transfer functions estimation of IM at deferent SCT fault level

7 SIMULATION OF TRANSIENT AND STEADY STATE BEHAVIOR OF IM

7.1 Modeling of IM in time domain

The mathematical model of induction motor with a rotor reference frame (*d, q*) can be described by nonlinear differential equations with four electrical variables, [stator currents (i_{ds}, i_{qs}) and rotor fluxes (φ_{dr}, φ_{qr})], a mechanical variable [rotor speed ω_r], and two control variables [stator voltages (V_{ds}, V_{qs})] [23-24]:

$$\begin{cases} V_{ds} = R_s i_{ds} + \frac{d\psi_{ds}}{dt} - \omega_r \psi_{qs} \\ V_{qs} = R_s i_{qs} + \frac{d\psi_{qs}}{dt} + \omega_r \psi_{ds} \\ 0 = R_r i_{dr_{(j=1,n)}} + \frac{d\psi_{dr_{(j=1,n)}}}{dt} \\ 0 = R_r i_{qr_{(j=1,n)}} + \frac{d\psi_{qr(j=1,n)}}{dt} \end{cases}, \tag{14}$$

with

$$\begin{cases} \psi_{ds} = (L_m + L_{\sigma s})\, i_{ds} + L_m i_{dr} \\ \psi_{qs} = (L_m + L_{\sigma s})\, i_{qs} + L_m i_{qr} \\ \psi_{dr} = (L_m + L_r)\, i_{dr} + L_m\, (i_{ds} + i_{dr}) \\ \psi_{qr} = (L_m + L_r)\, i_{qr} + L_m\, (i_{qs} + i_{qr}) \end{cases}. \tag{15}$$

The EC differential equations can be completed by the equation of motion expressed by (16) and (17):

$$J\frac{d\omega_r}{dt} = T_e - T_r - f_v \omega_r, \tag{16}$$

$$T_e = \frac{3}{2} P L_m\, (i_{qs} i_{dr} - i_{ds} i_{qr})\,, \tag{17}$$

with the motor inertia $J = 0.00375$ kgm^2, the kinetic friction coefficient $f_v = 0.00001$, the pole-pairs number

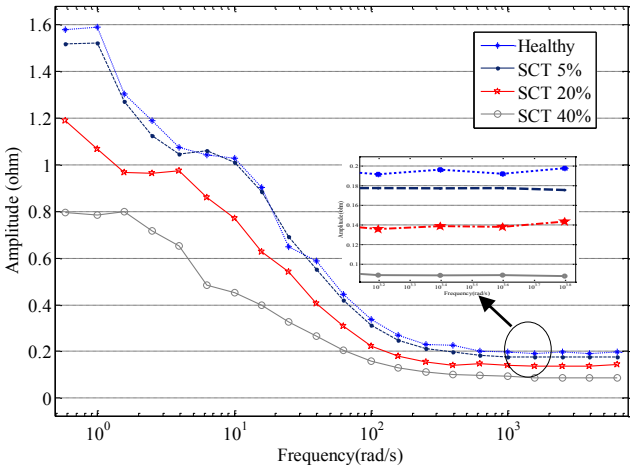

Fig. 7. OIN variation vs. faults severity

$P = 2$, T_e, T_r, the electromagnetic torque and load torque respectively. The simulation model is shown in Fig. 8.

7.2 Model validation based on free acceleration test

To verify the estimated model performance in actual operating conditions, the free acceleration test is performed. As shown in Fig. 9, the induction machine is started at no-load by applying three phase AC power, then the nominal load is applied.

During the acceleration and steady-state the stator phase current, the mechanical torque and rotor angular speed are measured using Cassy-Lab sensors.

Using the EC parameters cited in Table 2, the stator current, torque, and speed responses are simulated with the estimated second order EC model. The estimated model responses are compared to the measured responses.

In healthy condition stator current in Fig. 10, is shown to be symmetrical for the experimental test (Fig. 9). The amplitude of this current increases from 0.6 A at no-load to 0.8 A at full-load.

Figure 11 demonstrate the motor start-up from standstill to a steady speed of 1490 RPM at no-load and decreases to 1380 RPM at full-load, which demonstrate the effectiveness of the proposed model.

In the case of faulty scenario, figures 10-12 show the current, speed, and torque values, respectively influenced by fault degree, and load level. Compared to healthy IM.

The amplitude of stator current, speed, torque wave is evidently noticed when SCT fault arises in IM. These figures clearly show that the fault degree and load level play an important role in the variation of the of the motor variables amplitude.

To conclude, SCT fault extent changes and loading condition have a direct influence on the undulations of motor signals, (current, speed, and torque), and this impact including both frequency and amplitude, which had been detailed in the next section.

8 VALIDATION OF SCT MODELS BASED ON FFT ANALYSIS

8.1 Theoretical predictions

To develop a reliable diagnostic strategy it is highly important to identify the current components in the stator winding that are only a function of shorted turns.

As exposed in several preceding works, there have been many of published papers on the analysis of air-gap and axial flux signals to detect shorted turns [5-25].

Previous theoretical and experimental studies have demonstrated that the following equation gives the components in the air-gap flux waveform that are a function of shorted turns:

$$f_{sh}{=}f_{\mathrm{s}}\left[\mathrm{k}{\pm}\frac{n}{P}\ (1-g)\right], \tag{18}$$

where f_{sh} is the components that are a function of shorted turns, f_s is the supply frequency and n = integer 1, 2, 3, $k = 1, 3, 5$, P the pole-pairs, and g is the slip.

8.2 Simulation results using power spectrum

In order to validate the shorted turn model derived from SSFR test, the motor current signature analysis MCSA is used. The spectrum has been limited to a bandwidth of 500 Hz, to observe only low-frequency phenomena, and to limit the frequency-domain induction machine model to resistances, inductances, current, and voltage source.

8.2.1 Healthy motor

Initially, the IM at no load and at full load in healthy conditions is simulated, Fig.13-a shows the spectrum of stator current when the motor rotates at the rated speed, the fundamental amplitude is -9.148 dB (50 Hz). At full load become -6.739 dB (50 Hz). Noted that no harmonics are visible in the current spectrum.

8.2.2 5% Short-circuit of winding

The power spectrum of faulty IM with 5% short circuit at no load is given in Fig. 14-a, the fault frequencies appear at 25, and 75 Hz, with the indicative peak -93.83, and -110.3 dB, respectively.

At full load, fault frequencies appear at 27, and 73 Hz with the indicative peak -77.92 and -97.64 dB, respectively, as shown in Fig. 14-b. It gives an indication that the magnitude of fault frequency increases with increases in load. It is also observed from the figures that fault frequencies are clearly visible which indicates the SCT fault in IM.

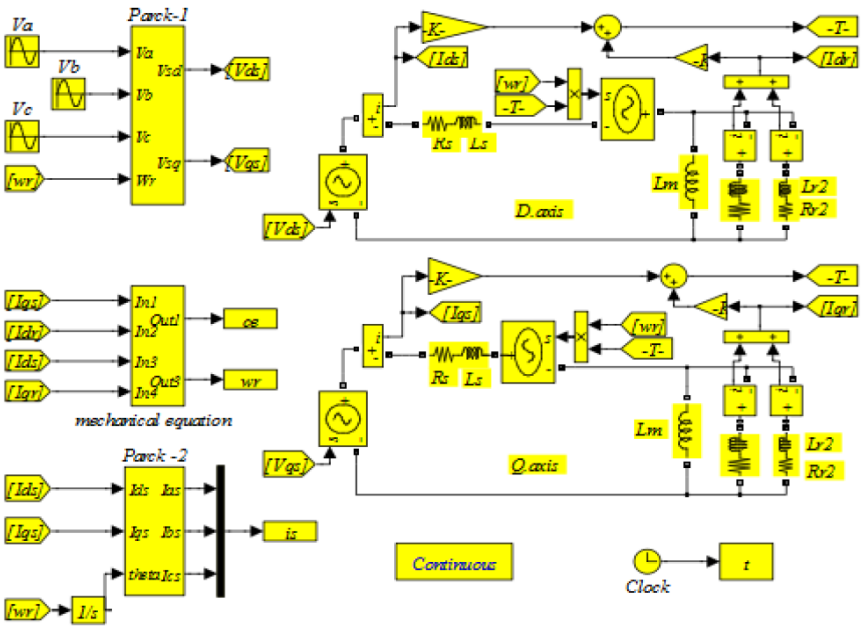

Fig. 8. Simulation block of IM from SSFR test

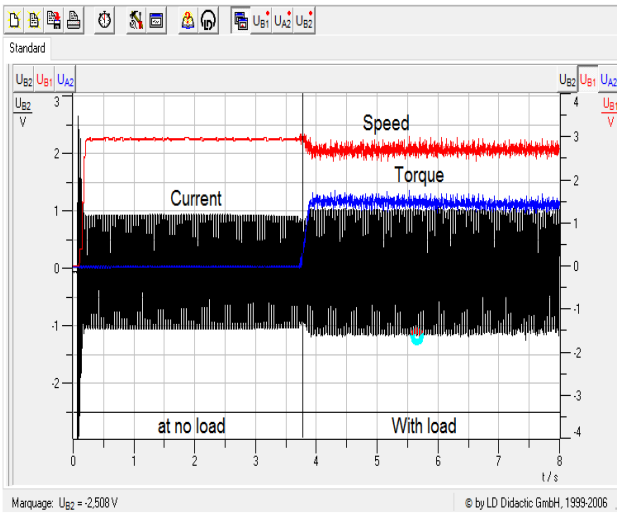

Fig. 9. Experimental characteristic of healthy IM

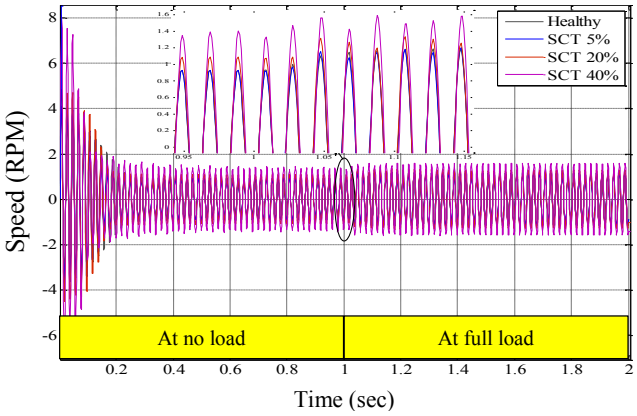

Fig. 10. Simulated current of healthy and faulty IM

8.2.3 20% Short-circuit of winding

The power spectrums of IM are also plotted for no load operating condition with increased severity of fault to 20%. As show Fig. 15-a, the SCT fault gives rise to some spectral components (25 Hz, -84.36 dB), (75 Hz, -87.87 dB).

The magnitude of fault frequencies has been increased if compared with the magnitude of 5% severity of faults.

For full load condition, the same consequence has been observed as shown in Fig. 15-b. The fault frequencies appear at (27 Hz, -69.11 dB), (73 Hz, -85.38 dB), which is also a calculated value at full load from (18). However, the magnitudes of this fault frequency have been significantly increased due to increased severity of the fault and loading condition.

8.2.4 40% Short-circuit of winding

The severity of the fault is increased by 40% and power spectrums for no load and full load condition are shown in the Fig. 16-a and Fig. 16-b, respectively, cause additional harmonic line currents components, at no load, (25 Hz, -74.46 dB), (75Hz, -75.67 dB), and at full load, (27 Hz,

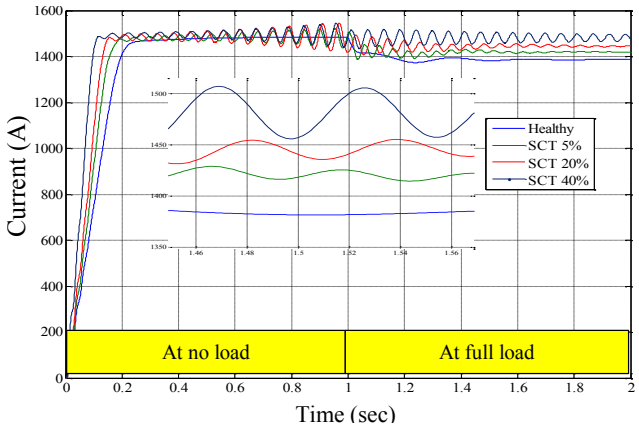

Fig. 11. Simulated speed of healthy and faulty IM

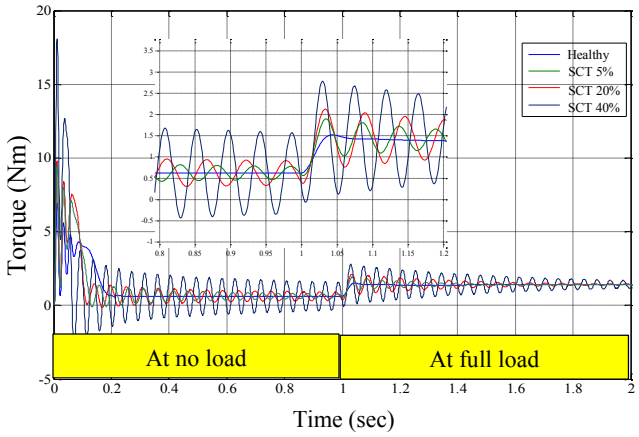

Fig. 12. Simulated torque of healthy and faulty IM

-53.13 dB), (73 Hz, -65.41 dB). It is observed from the figures that the magnitudes of fault frequencies have been significantly increased with increase of load and severity of faults.

The complete observation from power spectrum analysis for SCT fault is resumed in Table 3.

This results being in good agreement with the theoretical predictions, and simulation results presented before [26-27], which demonstrate the applicability of the proposed model in SCT fault modeling.

9 CONCLUSION AND PERSPECTIVES

This paper aims to develop an asymmetrical model of the SCT fault in the IM. The model is based on experimental parameter estimations from the stator voltage and current measured in a phase to phase of 250 W motor at standstill.

At the first time, the healthy IM is identified to obtain the EC model parameters, the performance of this model is verified by a comparison between the simulated characteristics (current, speed, and torque), and experimental results. Secondly, a real shorted turn fault is introduced using the fault simulator, and the parameters of the EC can be identified in a similar manner. Noted that as resulting of an SCT, the parameters of EC are varying (resistance, self-inductance, and mutual inductance) as a function of the fault severity.

The feasibility of using the standstill OIN for monitoring the level of shorted turns for induction motors has been shown in this paper. This method cannot offer continuous on-line monitoring, but it is sufficient to monitor SCT anomaly since the motor is stopped. Thus, it may be expected that in addition use in periodic maintenance.

Identified inter-turn models can be easily simulated and the electrical current has been analyzed. In order to validate the shorted turn model derived from SSFR test some power spectrum of the fault percentages and the healthy machine has been analyzed in order to compare with the theoretical predictions, and with the research results presented before, thus verifying the effectiveness of the proposed method.

An interesting perspective, which has not been explored in this paper because the space, is the effectiveness of the proposed method if we use a robust control structure for IM. The aim of this idea is to use the direct field oriented control (DFOC) which requires the knowledge of the electrical parameters, that guaranteed by the SSFR identification method proposed here.

DFOC can detect appearance of a fault in closed loop and switch itself between a nominal control strategy designed for healthy condition and robust control aimed for faulty one [7-28].

APPENDIX A APPENDIX SECTION

V_s	stator phase voltage
I_s	stator line current
$Z_s(j\omega)$	operational impedance
$L_s(j\omega)$	operational inductance
R_s	armature resistance
$L_{\sigma s}$	stator leakage inductance
L_m	magnetizing inductance
ψ_s	stator flux space vector
ψ_{ri}	rotor flux space vector of rotor branch
R_{ri}	stator referred resistance of rotor branch
$L_{\sigma ri}$	stator referred inductance of rotor branch
I_{ri}	rotor current space vector of rotor branch
I_r	rotor current space vector
I_m	magnetizing current space vector
ω	stator voltage angular velocity
ω_r	rotor angular velocity

Table 3. Power spectrum analysis of IM ender SCT fault at various load

Fig. no.	Fault severity	Load condition	Fault Frequencies			
			Lower side band		Upper side band	
			Frequency	Magnitude	Frequency	Magnitude
14. a	SCT 5%	No load	25 Hz	-93.83 dB	75 Hz	-110.3 dB
14. b	SCT 5%	Full load	27 Hz	-77.92 dB	73 Hz	-97.64 dB
15. a	SCT 20%	No load	25 Hz	-84.36 dB	75 Hz	-87.87 dB
15. b	SCT 20%	Full load	27 Hz	-69.11 dB	73 Hz	-85.38 dB
16. a	SCT 40%	No load	25 Hz	-74.46 dB	75 Hz	-75.67 dB
16. b	SCT 40%	Full load	27 Hz	-53.13 dB	73 Hz	-65.41 dB

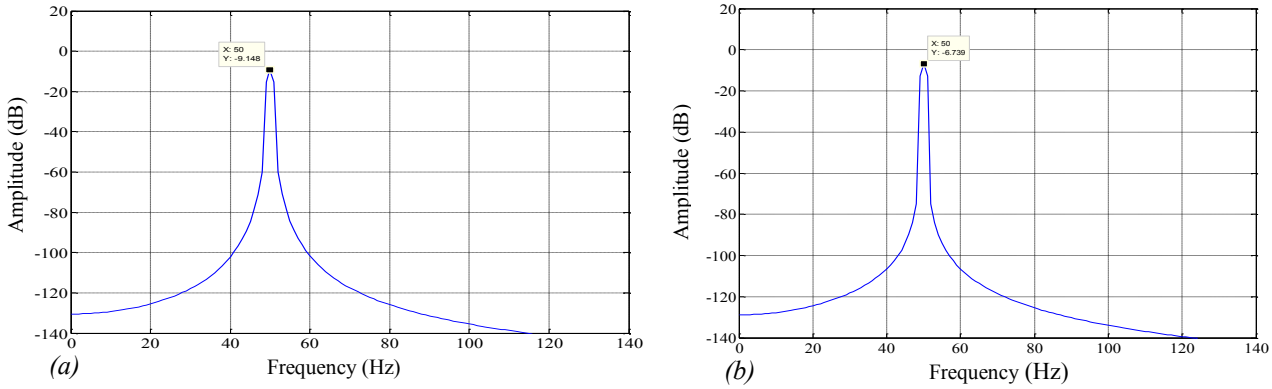

Fig. 13. Power spectrum of healthy IM at no load (a), and full load (b)

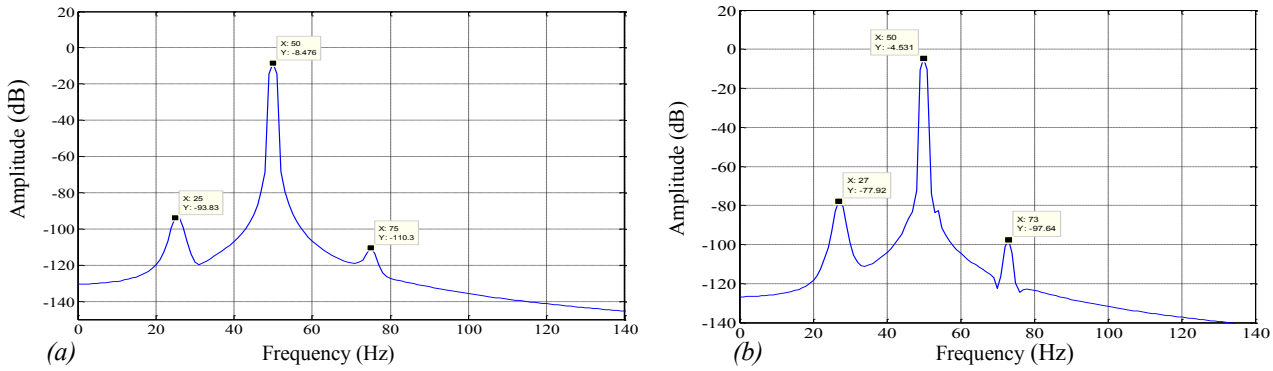

Fig. 14. Power spectrum of 5% faulty IM at no load (a), and full load (b)

REFERENCES

[1] P. Shi, Z. Chen, Y. Vagapov, Z. Zouaoui, "A new diagnosis of broken rotor bar fault extent in three phase squirrel cage induction motor," Mech Sys and Signal Processing, vol. 42, 2014, pp. 388–403.

[2] G. Jagadanand, L. Gopi, S. George, J. Jacob, "Inter-turn fault detection in induction motor using stator current wavelet decomposition," International Journal of Electrical Engineering and Technology (IJEET), Sep 2012, pp. 103-122.

[3] R. Roshanfekr, A. Jalilian, "Analysis of rotor and stator winding inter-turn faults in WRIM using simulated model and experimental results," Electric Power Systems Research, vol. 119, 2015, pp. 418–424.

[4] A. Lebaroud, A. Medoued, "Online computational tools dedicated to the detection of induction machine faults," Electrical Power and Energy Systems, vol. 44, 2013, pp. 752–757.

[5] G. M. Joksimovic, J. Penman, "The detection of inter-turn short circuits in the stator windings of operating motors," IEEE Transactions on Industrial Electronics, vol. 47, no. 5, 2000, pp.1087-1084.

[6] S. Bachir, S. Tnani, J.C. Trigeassou, G. Champenois,''Diagnosis by parameter estimation of stator and

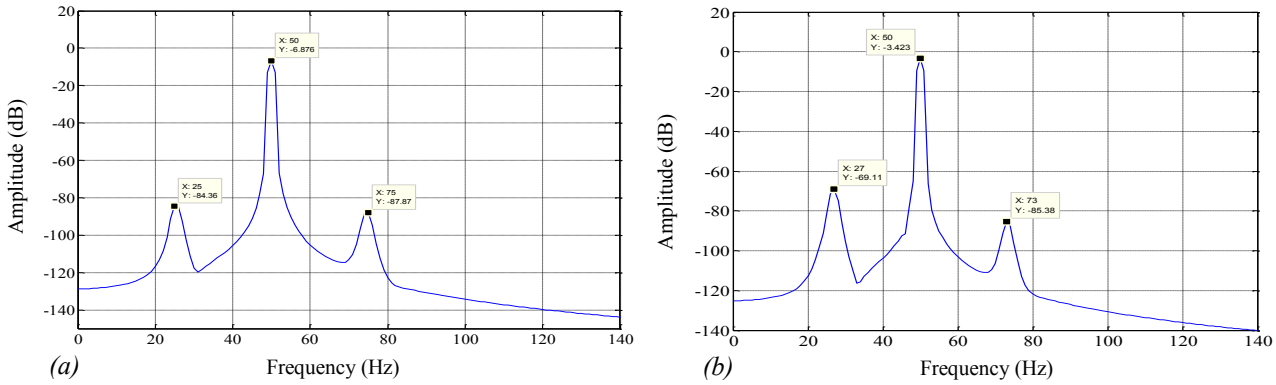

Fig. 15. Power spectrum of 20% faulty IM at no load (a), and full load (b)

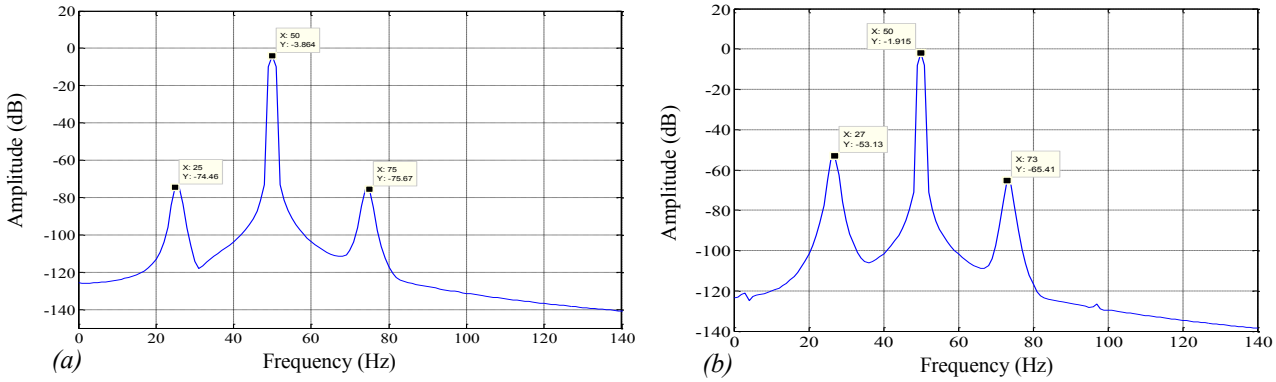

Fig. 16. Power spectrum of 40% faulty IM at no load (a), and full load (b)

rotor faults occurring in induction machines," IEEE Transactions on Industrial Electronics,vol. 53, no.3, Jun 2006, pp. 963-973.

[7] C.T. Kowalski, R. Wierzbicki, "Stator and rotor faults monitoring of the inverter-fed induction motor drive using state estimators," Automatika, vol. 54, no. 3, 2013, pp. 348–355.

[8] F. Duan, R. Zivanović, "Induction Motor Stator Fault Detection by a condition monitoring scheme based on parameter estimation algorithms," Electric Power Components and Systems, vol. 00, no. 0, 2016, pp. 1-11.

[9] P. J. Chrzan, G. Champenois, P. Coirault, and J. C. Trigeassou "Diagnosis of induction machine in standstill conditions," in Proc. SDPEMPED'99, 1999, pp. 497–501.

[10] C. Kral, F. Pirker, G. Pascoli, "Detection of rotor faults in squirrel-cage induction machines at standstill for batch tests by means of the vienna monitoring method," IEEE Transactions on Industry Applications, vol. 38, no. 3, May/June 2002, pp. 618-624.

[11] C. Demian, A. M. Mabwe, H. Henao, "Detection of induction machines rotor faults at standstill using signals injection," IEEETtransactions on Industry Applications, vol. 40, no. 6, Nov/Dec 2004, pp.1550-1559.

[12] Z. E. Gketsis, M.E. Zervakis, G.Stavrakakis, "Detection and classification of winding faults in windmill generators using wavelet transform and ANN," Electric Power Systems Research vol. 79, 2009, pp. 1483–1494.

[13] R. M. Tallam, T. G. Habetler, and R. G. Harley, "Transient model for induction machines with stator winding turn faults," IEEE Transactions on Industry Applications, vol. 38, no. 3, May/Jun 2002.

[14] G. B. Kliman, W. J. Premerlani, "Sensitive, on-line turn-to-turn fault detection in AC motors," Electric Machines & Power Systems, vol. 28, 2000, pp. 915–927,

[15] M. Arkan, D. K.Perovic, P.J. Unsworth, "Modelling and simulation of induction motors with inter-turn faults for diagnostics," Electric Power System Research , vol. 75, 2005, pp. 57–66.

[16] M. Bouzid, G. Champenois, "An efficient simplified multiple-coupled circuit model of the induction motor aimed to simulate different types of stator faults," Mathematics and Computers in Simulation, vol. 90, 2013, pp. 98–115.

[17] M. Hasni, O.Touhami, "Synchronous machine parameter estimation by SSFR test," Journal of Electrical Engineering, vol. 59, no. 2, 2008, pp. 75–80.

[18] S. I. Moon, A. Keyhani, "Estimation of induction machine parameters from standstill time-domain data," IEEE Transactions on Industry Applications, vol. 30, no. 6, Nov/Dec 1994.

[19] I. M. Canay, "Determination of the model parameters of machines from the reactance operator (evaluation of SSFR test)," IEEE Transaction on Energy Convertion vol. 8, no. 2, Jun 1993.

[20] IEEE Std. 115-1995, "IEEE guide procedures for synchronous machines, recognized as an American National Standard (SNSI)," 1995.

[21] J. R. Willis, G. J. Brock, and J. S. Edmonds, "Derivation of induction motor models from SSFR test," IEEE Transactions on Energy Convertion, vol. 4,no. 4, Dec 1989.

[22] F. R. Blánquez, C.A. Platero, E. Rebollo, F. Blázquez, "Field-winding fault detection in synchronous machines with static excitation through frequency response analysis," Electrical Power and Energy Systems, vol. 73, 2015, pp. 229–239.

[23] R. Nicolas, I. Marcel, D. Demba, "Modeling and experimental study of 3-phase short-circuits of a double-cage induction machine," Electrical Mmachines and Power System, vol. 27, 1999, pp. 343–362.

[24] A. Mabrek, K. E. Hemsas, "Transient operation modeling of induction machine using standstill frequency response test," IEEE conf publication, Dec. 2015, ICEE Algeria.

[25] J. Penman, H. G. Sedding, B. A. Lloyd, and W. T. Fink, "Detection and location of inter-turn short circuits in the stator windings of operating motors," IEEE Transactions on Energy Conversion, vol 9, no 4, Dec 1994.

[26] S. Nandi, H. A. Toliyat, and X. Li," Condition Monitoring and Fault Diagnosis of Electrical Motors—A Review," IEEE Transactions on Energy Conversion, vol. 20, no. 4, Dec 2005.

[27] N. Mehala, Condition monitoring and fault diagnosis of IM using MCSA. PhD thesis, National Institue of Technolology, India Electrical Engineering Departement, 2010.

[28] A. M. Guichiche, S. M. Boucherit, "An improved stator winding fault tolerance architecture for vector control of IM: Theory and experiment," Electric Power Systems Research, vol. 104, 2013, pp. 129–137.

Abdelhakim Mabrek was born in Bordj Bouarreridj, Algeria in 1983. He received his engineering and magister degrees from the University of Setif 1, Algeria in 2006 and 2011, respectively. Currently, he is employed as a laboratory engineer in electrical machine laboratory of Bordj Bouarreridj University and a member of the Automatic Laboratory of University of Setif, Algeria, where he is preparing his Ph.D. His main fields of interest are the induction motor drive control and state variable estimation, and its application for diagnostic problems of AC electrical drives.

Kamel E. Hemsas was born in Setif, Algeria. He received his engineering, magister and doctorate degrees from the University of Setif 1 Algeria in 1991, 1995 and 2005, respectively. His is a full professor in Electrical Engineering Department, and head of research at the same university. His areas of interest include on power quality issues, modeling, control diagnosis and state observer of electric machine and systems, renewable energy and artificial intelligence. He is the author of several international publications, communications and two books.

AUTHORS' ADDRESSES
Abdelhakim Mabrek, M.Sc.
Prof. Kamel E. Hemsas, Ph.D.
Automatic Laboratory of Setif Electrical Engineering Department,
University Ferhat Abbas Setif 1,
Route de Béjaia, Cité Maabouda, DZ-19000, Setif, Algeria
email: mabrekhakim@yahoo.fr,
hemsas.kamel@gmail.com

Received: 2016-05-23
Accepted: 2017-02-13